

## Effectiveness of design procedures for linear TMD installed on inelastic structures under pulse-like ground motion

Giuseppe Quaranta<sup>1a</sup>, Fabrizio Mollaioli<sup>\*2</sup> and Giorgio Monti<sup>2b</sup>

<sup>1</sup>Department of Structural and Geotechnical Engineering, Sapienza University of Rome, via Eudossiana 18, 00184 Rome, Italy

<sup>2</sup>Department of Structural and Geotechnical Engineering, Sapienza University of Rome, via Gramsci 53, 00197 Rome, Italy

(Received December 30, 2014, Revised October 1, 2015, Accepted October 12, 2015)

**Abstract.** Tuned mass dampers (TMDs) have been frequently proposed to mitigate the detrimental effects of dynamic loadings in structural systems. The effectiveness of this protection strategy has been demonstrated for wind-induced vibrations and, to some extent, for seismic loadings. Within this framework, recent numerical studies have shown that beneficial effects can be achieved by placing a linear TMD on the roof of linear elastic structural systems subjected to pulse-like ground motions. Motivated by these positive outcomes, closed-form design formulations have been also proposed to optimize the device's parameters. For structural systems that undergo a near-fault pulse-like ground motion, however, it is unlikely that their dynamic response be linear elastic. Hence, it is very important to understand whether such strategy is effective for inelastic structural systems. In order to provide new useful insights about this issue, the paper presents statistical results obtained from a numerical study conducted for three shear-type hysteretic (softening-type) systems having 4, 8 and 16 stories equipped with a linear elastic TMD. The effectiveness of two design procedures is discussed by examining the performances of the protected systems subjected to 124 natural pulse-like earthquakes.

**Keywords:** inelastic structure; optimization; pulse-like ground motion; tuned mass damper

---

### 1. Introduction

The placement of tuned mass dampers (TMDs) within structural systems can be a viable approach for mitigating undesirable effects induced by dynamic loadings. Active or semi-active TMDs provide a flexible and adaptive vibration control strategy (Lin *et al.* 2013) whereas passive TMDs are especially attractive for their robustness, easy maintenance and reduced manufacturing costs. For instance, Kwok and Samali (1995) studied the effectiveness of passive and active TMDs for linear single-degree-of-freedom (SDOF) system under wind loads. Liu *et al.* (2008) have extended the analysis to a linear multi-degrees-of-freedom (MDOF) system taking into account the

---

\*Corresponding author, Associate Professor, E-mail: [fabrizio.mollaioli@uniroma1.it](mailto:fabrizio.mollaioli@uniroma1.it)

<sup>a</sup>Assistant Professor, E-mail: [giuseppe.quaranta@uniroma1.it](mailto:giuseppe.quaranta@uniroma1.it)

<sup>b</sup>Full Professor, E-mail: [giorgio.monti@uniroma1.it](mailto:giorgio.monti@uniroma1.it)

soil-structure interaction. On the other hand, Li and Hu (2002) proposed the application of TMDs for reducing fatigue damages. Existing studies seem to be conclusive about the usefulness of TMDs in reducing vibrations due to wind action if the protected system exhibits a linear elastic behavior, a realistic situation for buildings under serviceability conditions. Researches about the effectiveness of TMDs in seismic protection are more recent, but encompass a significant number of relevant issues. Marano *et al.* (2007), Marano and Quaranta (2009), Chakraborty and Roy (2011) have presented optimal design methods for protecting linear elastic structural systems subjected to seismic ground motion by means of passive TMD, where the main focus was the development of proper strategies for handling probabilistic or non-probabilistic uncertainties within the framework of random vibration theory. The use of passive TMDs for reducing the seismic response of irregular buildings was presented in (Lin *et al.* 2000) whereas Hoang *et al.* (2008) have studied the optimum design of a TMD for the seismic retrofitting of a long-span truss bridge. When assessing the effectiveness of linear TMDs in reducing the displacement response of elastic systems subjected to 52 components of ground motion records (from 26 earthquakes), Sadek *et al.* (1997) observed that:

- a greater reduction is achieved for smaller values of the structural damping,
- the larger is the ratio between the TMD's mass and the mass of the protected system (this ratio was considered in the range 0.02-0.10), the greater are its effectiveness and the dispersion of the results,
- TMDs are not effective for structures with short natural vibration periods (i.e. structures with periods 0.1-0.2 s),
- the mean of the displacement ratio of the protected structure with and without TMD ranges from 0.75 to 0.95, whereas the coefficient of variation of this ratio ranges from 0.05 to 0.15.

Despite the amount of existing studies, the effectiveness of TMDs against seismic loading seems still a debated topic. Existing difficulties can be traced back to the high sensitivity of the TMD's performance with respect to the characteristics of soil, foundations and seismic excitation as well as to the way by which the structural system is modeled. For this reason, in recent installations of TMDs, the possibility for on-site tuning has been foreseen. Wu *et al.* (1999) have pointed out that soil-structure interaction can play an important role in determining the effectiveness of TMDs for seismic applications. They showed that strong soil-structure interaction defeats the seismic effectiveness of TMD systems. Moreover, they noticed that a TMD can hardly reduce the seismic response of a structure supported on shallow spread footings and underlying soft soil. Such conclusions were drawn for linear structural systems subjected to stationary random excitations. Lee *et al.* (2012) have studied the effectiveness of TMDs in reducing seismic risk for inelastic systems subjected to real earthquake records. When a linear elastic TMD is designed according to a simplified approach (i.e., TMD's optimal parameters are estimated by considering the linear elastic properties of the protected building), they found that the ratio between the peak displacement of the structure with TMD and the peak displacement of the unprotected structure (both normalized by the corresponding yield displacement) can be larger than 1 (up to 1.4 for an approximate bilinear system). This implies that a linear elastic TMD designed according to such simplified procedures may sensibly worsen the structural performance under some seismic events. This evidence was already pointed out in (Sgobba and Marano 2010), where the optimum parameters of the TMD were obtained with a numerical procedure once the hysteretic protected system was linearized in a stochastic sense. Particularly, they also concluded that the use of a linear TMD does not appear useful for displacement-control of inelastic structures subjected to stationary Kanai-Tajimi stochastic ground motion. According to Pinkaew *et al.* (2003), available

results demonstrate that TMDs become effective in reducing the seismic response of structures only when the ground motion exhibits narrow-band frequency and long duration, see also (Lukkunaprasit and Wanitkorkul 2001). Recently, Matta (2013) has shown that - under certain conditions - a linear TMD can be also effective in reducing the seismic demands in linear elastic systems subjected to pulse-like ground motion. Within this lively debate, the effectiveness of TMDs against pulse-like ground motions appears a critical issue that deserves further studies. In this perspective, while the linear elastic behavior might be a reasonable approximation for moderate far-field seismic events, it is not a realistic model for structural systems subjected to near-fault earthquakes. Additionally, it should be remarked that near-fault earthquakes occur with seismological characteristics markedly different from than those observed for far-field seismic events. In fact, a comprehensive number of strong motion records obtained in recent earthquakes at sites close to the seismic causative fault were characterized by noticeable variability in the damage potential (Mavroeidis and Papageorgiou 2003, Bray and Rodriguez-Marek 2004, Mollaioli *et al.* 2006, Kalkan and Kunnath 2006, Baker 2007). The reasons of this variability are the proximity of the source and the occurrence of forward directivity effects. Forward directivity refers to the strengthening of ground motion at sites located in the direction of the predominant rupture propagation, because it produces strong motions near the earthquake ruptures that have often a pulse-like waveform. Specifically, most of the energy originating from the source develops in a coherent, high-velocity pulse of moderate-to-long duration, with the strongest motion usually polarized in the direction normal to the fault (Hall *et al.* 1995).

In order to provide new insights and recommendations, this paper addresses the effectiveness of optimum design procedures for linear TMD installed on inelastic structures subjected to pulse-like ground motion. The numerical analysis of three shear-type hysteretic (softening-type) systems having 4, 8 and 16 stories equipped with a linear elastic passive TMD is presented. The device is designed according to two closed-form procedures in which the elastic properties of the protected buildings are considered, and a statistical analysis has been performed on a database consisting of 124 natural accelerograms.

## 2. Structural model and optimum TMD design

### 2.1 Inelastic building with roof-type linear TMD

A simplified model is adopted to represent the inelastic behavior of the structural systems. It is assumed that they can be modeled as hysteretic MDOF shear-type systems, for which (by omitting the time variable) the nonlinear dynamic equations can be defined in the following form

$$\mathbf{M}\ddot{\mathbf{x}} + \mathbf{C}\dot{\mathbf{x}} + \mathbf{K}\mathbf{x} + \mathbf{H}\mathbf{z} = -\mathbf{M}\mathbf{r}\ddot{x}_g, \quad (1)$$

where  $\mathbf{M}$  is the mass matrix,  $\mathbf{C}$  is the viscous damping matrix,  $\mathbf{K}$  is the elastic stiffness matrix and  $\mathbf{H}$  is the matrix that contains the nonlinear (hysteretic) terms,  $\mathbf{r}$  is the influence vector and  $x_g$  is the ground displacement (the upper dot indicates the time derivative). The system matrices in Eq. (1) have the following form

$$\mathbf{M} = \text{diag}\{m_1 \quad \cdots \quad m_i \quad \cdots \quad m_N\}, \quad (2)$$

$$\mathbf{C} = \begin{bmatrix} c_1 + c_2 & -c_2 & & & & \\ -c_2 & c_2 + c_3 & -c_3 & & & \\ & & \ddots & & & \\ & & & -c_{N-1} & c_{N-1} + c_N & -c_N \\ & & & & -c_N & c_N \end{bmatrix}, \quad (3)$$

$$\mathbf{K} = \begin{bmatrix} \alpha_1 k_1 + \alpha_2 k_2 & -\alpha_2 k_2 & & & & \\ -\alpha_2 k_2 & \alpha_2 k_2 + \alpha_3 k_3 & -\alpha_3 k_3 & & & \\ & & \ddots & & & \\ & & & -\alpha_{N-1} k_{N-1} & \alpha_{N-1} k_{N-1} + \alpha_N k_N & -\alpha_N k_N \\ & & & & -\alpha_N k_N & \alpha_N k_N \end{bmatrix}, \quad (4)$$

$$\mathbf{H} = \begin{bmatrix} (1-\alpha_1)k_1 & -(1-\alpha_2)k_2 & & & & \\ & (1-\alpha_2)k_2 & -(1-\alpha_3)k_3 & & & \\ & & \ddots & & & \\ & & & & (1-\alpha_{N-1})k_{N-1} & -(1-\alpha_N)k_N \\ & & & & & (1-\alpha_N)k_N \end{bmatrix}, \quad (5)$$

where  $i=1, \dots, N$  indicates the  $i$ th floor level,  $k_i$  is the initial stiffness value at the  $i$ th floor level,  $m_i$  is the  $i$ th floor mass,  $\alpha_i$  is a weighting constant representing the relative participations of the linear and nonlinear terms ( $0 \leq \alpha_i \leq 1$ ). Therefore, if  $\alpha_i \rightarrow 1$ , then the role of the corresponding nonlinear term becomes negligible. The symbol  $\mathbf{x}$  in Eq. (1) collects the relative displacements of the  $i$ th mass with respect to the ground. Inter-storey drifts (the relative displacements between floors) are denoted as  $d_i = x_i - x_{i-1}$  for  $i \neq 1$  and  $d_1 = x_1$ . The vector  $\mathbf{z}$  in Eq. (1) collects the so-called hysteretic displacements. It is assumed that the hysteretic behavior of the  $i$ th mass depends on the relative displacement between floors  $d_i$ , according to the Bouc-Wen model

$$\dot{z}_i = A_i d_i - \beta_i \left| \dot{d}_i \right| \left| z_i \right|^{n_i-1} z_i - \gamma_i \dot{d}_i \left| z_i \right|^{n_i}, \quad (6)$$

where  $\beta_i$ ,  $\gamma_i$  and  $n_i$  are hysteresis shape parameters. The relative values of  $\beta_i$  and  $\gamma_i$  determine the type of nonlinear response, i.e., softening or hardening (for a weakly softening response,  $\beta_i + \gamma_i > 0$  and  $\gamma_i - \beta_i < 0$ ). The parameter  $A_i$  has been demonstrated to be redundant, and thus it is assumed equal to 1. The parameter  $\alpha_i$  is the ratio between the post-yield tangent stiffness and the initial stiffness. The parameter  $n$  controls the smoothness of cycle. For  $n \rightarrow \infty$ , the model approaches to a bilinear one. The motion equation given by Eq. (1) is solved assuming zero initial conditions. When a linear elastic TMD is placed on the top of the building,  $N$  refers to the structural degree-of-freedom (DOFs) plus the SDOF corresponding to the TMD. In this case, the last equation is modified accordingly, i.e., by removing the hysteretic contribution. Once the mass  $m_i$  and the initial stiffness  $k_i$  of the structure are known, the matrices  $\mathbf{K}$  and  $\mathbf{M}$  can be obtained as in Eqs. (4), (5). The matrix  $\mathbf{C}$  in Eq. (3) is obtained by specifying the viscous damping ratio for each mode  $\zeta_i$ , where  $c_i/m_i = 2\zeta_i\omega_i$  and  $\omega_i^2 = k_i/m_i$ . The interested reader is referred, for instance, to (Ikhouane and Rodellar 2007) and (Ikhouane *et al.* 2007) for more details about the dynamics of the Bouc-Wen model.

### 2.2 Optimum parameters of the TMD

It is now addressed the problem of designing a linear elastic TMD installed on the roof of a multi-storey building. Two methods are considered, in which the elastic properties of the protected building are required to calculate the device's parameters. Both methods allow the determination of the optimal frequency ratio  $\Omega_{TMD}$  (the optimal ratio of the TMD natural frequency to the target structural natural frequency) and the TMD damping ratio  $\xi_{TMD}$  once the structural damping and the TMD's mass are given. The TMD's mass is considered by introducing the dimensionless parameter  $\mu_{eff}$ . For a SDOF,  $\mu_{eff}$  is the ratio between the TMD's mass the mass of the protected system. For a MDOF system, the mass ratio equivalence proposed in (Warburton 1982) can be applied if the target mode of the protected system (usually its first mode) is far from other modes. In this case,  $\mu_{eff}$  is the ratio of the TMD's mass to the effective modal mass of the target mode (in this study, it is the first vibration mode).

The first method is the  $H_\infty$ -based design. It aims at minimizing the  $H_\infty$  norm of the acceleration-to-displacement transfer function. This corresponds to the minimization of the steady-state structural displacement amplitude under a harmonic-type acceleration time history having constant amplitude and any possible frequency content. For a structural damping ratio equal to 0.02,  $H_\infty$ -based design leads to the following formulations (Matta 2013)

$$\Omega_{TMD} = \frac{\Omega_{TMD,0}}{1 + a_1\sqrt{\mu_{eff}} + a_2\mu_{eff}^3}, \tag{7}$$

$$\xi_{TMD} = \xi_{TMD,0} + a_3 - a_4\mu_{eff}^2, \tag{8}$$

where

$$\Omega_{TMD,0} = \frac{\sqrt{1 - \mu_{eff}/2}}{1 + \mu_{eff}}, \tag{9}$$

$$\xi_{TMD,0} = \sqrt{\frac{3\mu_{eff}}{8(1 + \mu_{eff})(1 - \mu_{eff}/2)}}, \tag{10}$$

in which  $a_1=0.04758$ ,  $a_2=0.03056$ ,  $a_3=0.002715$ , and  $a_4=0.007453$ . The second method is indicated as  $H_p$ , and it has been specifically presented in (Matta 2013) to deal with pulse-like ground motion. For a structural damping ratio equal to 0.02 and by taking into account an average pulse, the following formulations can be used

$$\Omega_{TMD} = \frac{\Omega_{TMD,0}}{1 + b_1\sqrt{\mu_{eff}} + \mu_{eff}^3 \left[ b_2 - b_3 / (1 + b_4\mu_{eff}^5) \right]}, \tag{11}$$

$$\xi_{TMD} = \frac{b_5\mu_{eff}^4 - b_6\mu_{eff}^3 + b_7\mu_{eff}^2 - b_8\mu_{eff}}{\mu_{eff}^3 - b_9\mu_{eff}^2 - b_{10}\mu_{eff} + b_{11}}, \tag{12}$$

where  $b_1=0.2926$ ,  $b_2=0.2301$ ,  $b_3=75.34$ ,  $b_4=30185$ ,  $b_5=0.7269$ ,  $b_6=0.3934$ ,  $b_7=0.07388$ ,  $b_8=0.001194$ ,  $b_9=0.2978$ ,  $b_{10}=0.01214$ ,  $b_{11}=0.01407$ . The coefficients that appear in Eqs. (7)-(12)

are obtained by regression of numerical results, and thus their value is referred to a structural damping ratio equal to 0.02.

### 3. Numerical analysis

#### 3.1 Database of pulse-like ground motion records

A database of 124 natural pulse-like earthquake records has been used to estimate the performance of three inelastic shear-type systems equipped with a linear TMD. In doing so, it should be highlighted that one of the primary factors affecting the motion in the near-fault region is the direction in which rupture progresses from the hypocenter along the zone of rupture. A site may be categorized subsequently to an earthquake as representing forward, reverse, or neutral directivity effects (Somerville and Graves 1993, Hall *et al.* 1995, Somerville *et al.* 1997). If the rupture propagates toward the site, then it is likely to demonstrate forward directivity. If rupture propagates away from the site, then it will likely exhibit backward directivity. If the site is more or less perpendicular to the fault from the hypocenter, then it will likely demonstrate neutral directivity. Therefore, the selected ground motions were recorded in regions prone to forward directivity effects and satisfy the geometric conditions for forward directivity. In addition, the velocity time histories of these ground motions show a polarization in the fault-normal direction and are characterized by a clear pulse in the fault-normal direction. Consequently, the two horizontal components of the ground motions were projected in the fault-parallel (FP) and the fault-normal (FN) direction. Pulse-like records due to soft soil site effects or other effects are not considered. The larger fault-normal component of motion is considered critical and is commonly used for structural analyses. In fact, the presence of high amplitude, long duration pulses in near-field ground motions gives rise to considerable velocity and displacement demands, and it can be consequently considered as a key issue in producing damage, due to the transmission of large amounts of energy that should be dissipated in a short time (Mollaioli *et al.* 2006, Mollaioli and Bosi 2011). About the soil classification at recording stations, with the exception of 4 ground motions recorded on soil type B (according to the NEHRP site classification based on the  $V_{S30}$  value), all the others ground motions were recorded on soil type C or D. The magnitude of all earthquakes ranges from 5 to 7.6. Moreover, with the aim of underlining the effect of the pulses on the performance of the structures equipped with TMD, the pulse-like ground motions have been grouped into bins of pulse period  $T_p$ . The pulse periods have been calculated according to the procedure suggested by Baker (2007) for all the records considered. The earthquake magnitude  $M$  and the corresponding pulse period  $T_p$  in [s] of the selected seismic events are shown in Fig. 1. The complete list of the earthquakes from which these near-fault pulse-like ground motions were recorded is reported in Appendix A (see Table A.1). Further details about this database can be found in (Mollaioli *et al.* 2014).

#### 3.2 Structural systems

Three shear-type inelastic structural systems with 4, 8 and 16 stories are considered. A constant viscous damping ratio equal to 0.02 is assumed. The mass is constant for all floors and a linear variation of the elastic stiffness is assumed, where the last floor has an elastic stiffness obtained by reducing the elastic stiffness of the first floor (this reduction is assumed equal to 30%). For the

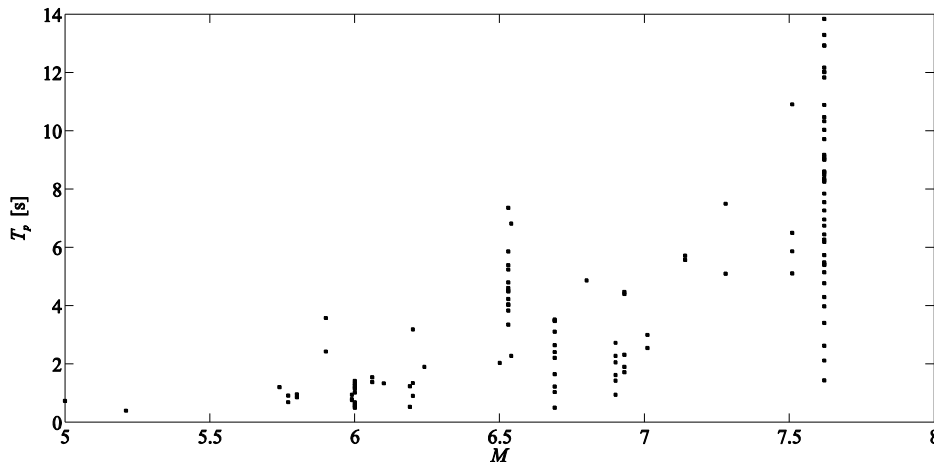


Fig. 1 Relationship between pulse period  $T_p$  [s] and earthquake magnitude  $M$  within the considered set of pulse-like ground motion records

Table 1 First three elastic periods ( $T_1, T_2, T_3$ ) in [s] and the ratio of the TMD mass to the effective modal mass of the target mode  $\mu_{eff}$

DOF	$T_1$ [s]	$T_2$ [s]	$T_3$ [s]	$\mu_{eff}$
4	1.0783	0.3861	0.2527	0.5693
8	2.0289	0.7010	0.4313	0.2962
16	3.4687	1.2010	0.7272	0.1530

sake of uniformity, the parameters of the Bouc-Wen model are the same for all systems and are constant for all floors (therefore, the subscript  $i$  is omitted hereafter). A weakly softening behavior is simulated, and  $n$  is equal to 1.01. For each MDOF system, the ratio between the TMD mass and the mass of the last floor is 2. This can be considered a heavy TMD. A linear elastic model is assumed for the TMD. The first three elastic periods ( $T_1, T_2, T_3$ ) of the structural systems are listed in Table 1 together with  $\mu_{eff}$ , i.e., the ratio of the TMD's mass to the effective modal mass of the target mode (the first elastic mode).

It can be observed that the target mode is sufficiently far from other modes, and thus the mass ratio equivalence proposed in (Warburton 1982) can be applied. By keeping constant the ratio between the TMD mass and the mass of the last floor, it is also evident that the larger the number of DOF, the smaller the value  $\mu_{eff}$ . This, in turn, allows the assessment of the role of the TMD's mass with respect to the effective modal mass of the target mode.

Two performance indices are examined to evaluate the effectiveness of the TMD design procedures. They are

$$I_d = \frac{\|\mathbf{d}_{max}\|}{\|\mathbf{d}_{max}^0\|}, \tag{13}$$

$$I_a = \frac{\|\mathbf{a}_{max}\|}{\|\mathbf{a}_{max}^0\|}, \tag{14}$$

where the symbol  $\|\cdot\|$  indicates the Euclidean norm, the vectors  $\mathbf{d}_{max}$  and  $\mathbf{a}_{max}$  collect the maximum absolute inter-storey drift values and the maximum absolute floor accelerations of the protected

system, respectively, whereas the superscript 0 applies to the quantities evaluated without the TMD. The main scope behind the use of such indices is that of assessing the effectiveness in reducing structural damages (related to the inter-storey drift) and non-structural damages in equipment and furniture (caused by high acceleration levels). The analyses have been performed by means of MATLAB (2013b) wherein Eq. (2) has been integrated using the Runge-Kutta 4th/5th-order method (*ode45* embedded MATLAB function).

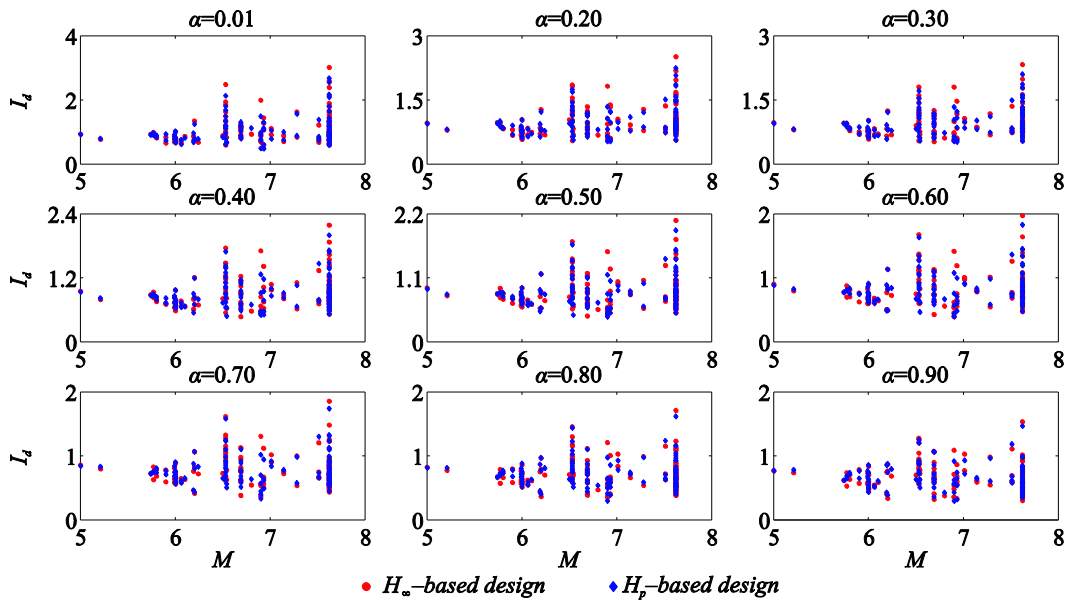


Fig. 2 Results for 4 DOF system ( $T_1=1.0783$  s): relationship between  $I_d$  and  $M$  for different values of  $\alpha$

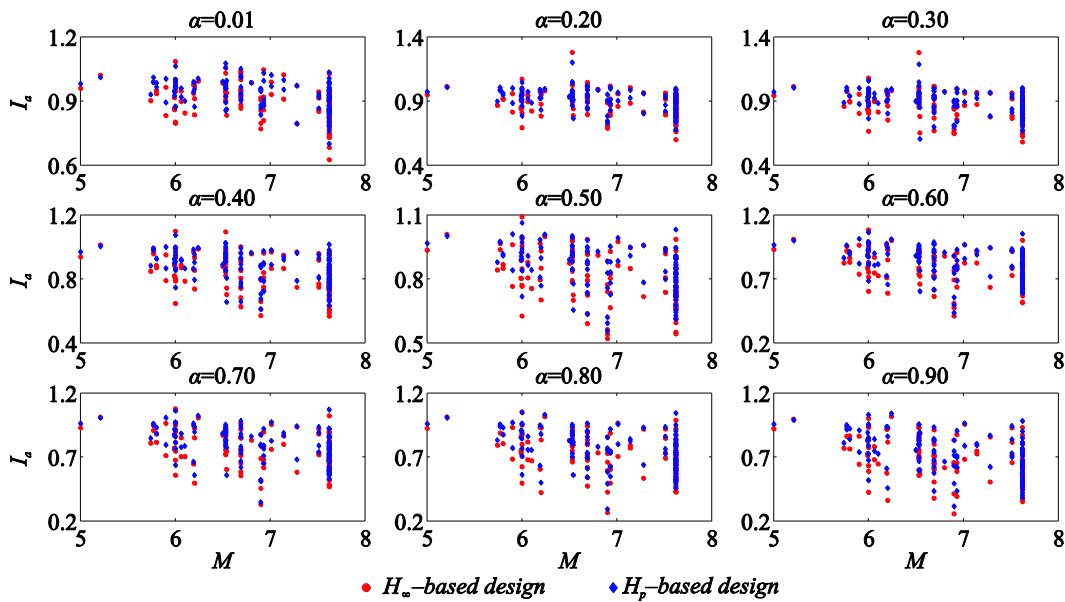


Fig. 3 Results for 4 DOF system ( $T_1=1.0783$  s): relationship between  $I_a$  and  $M$  for different values of  $\alpha$

### 3.3 Results

Numerical values of  $I_d$  and  $I_a$  for 4, 8 and 16 DOF systems are shown from Fig. 2 to Fig. 13 by considering different values of  $\alpha$ . These figures include the results obtained by means of, both,  $H_\infty$ - and  $H_p$ -based design. The values of the performance indices are plotted with respect to the earthquake magnitude  $M$  and to the pulse period  $T_p$  in [s] in order to look for possible correlations between structural performance and seismological parameters.

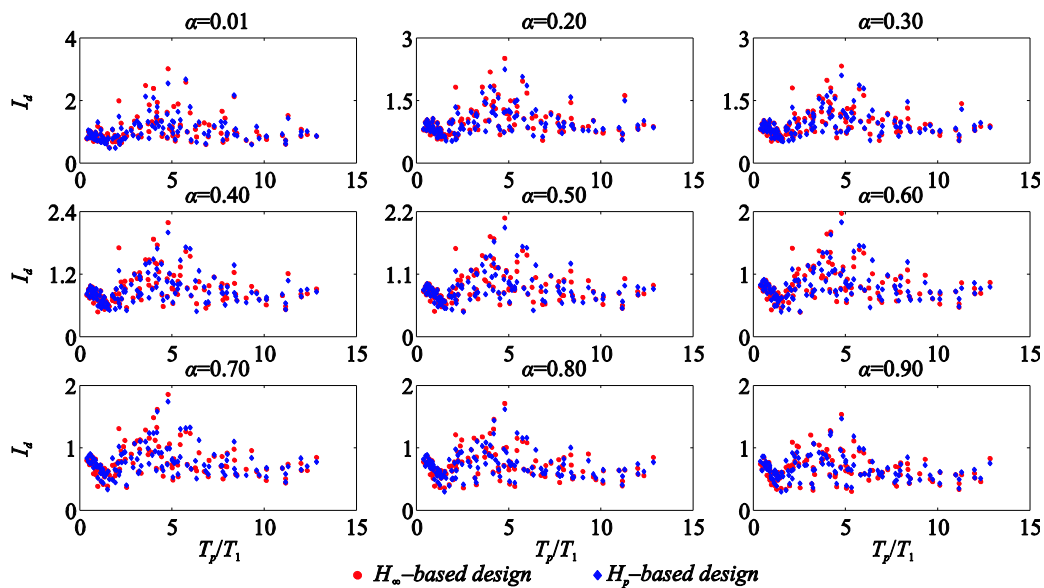


Fig. 4 Results for 4 DOF system ( $T_1=1.0783$  s): relationship between  $I_d$  and  $T_p/T_1$  for different values of  $\alpha$

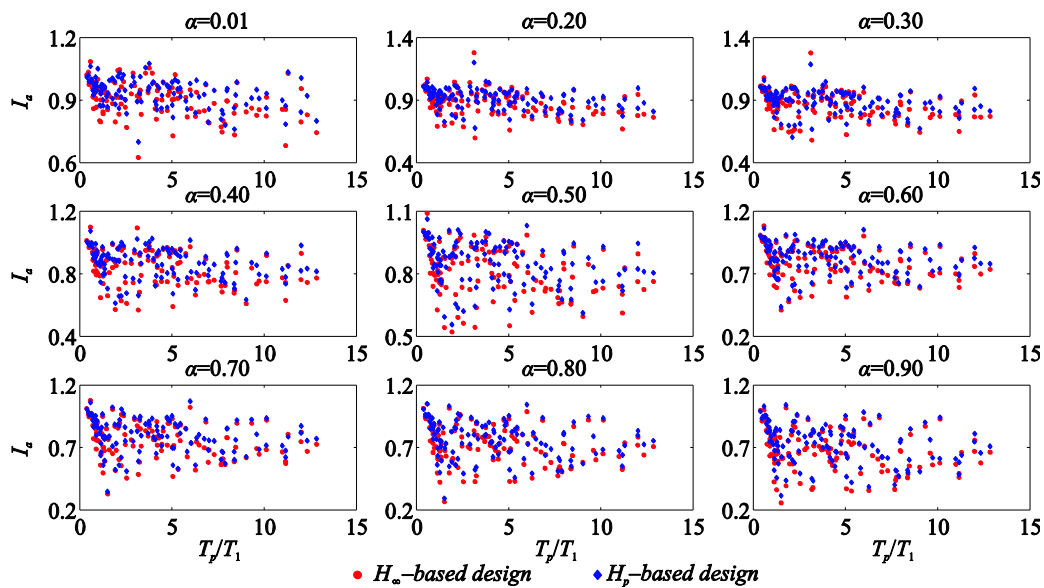


Fig. 5 Results for 4 DOF system ( $T_1=1.0783$  s): relationship between  $I_a$  and  $T_p/T_1$  for different values of  $\alpha$

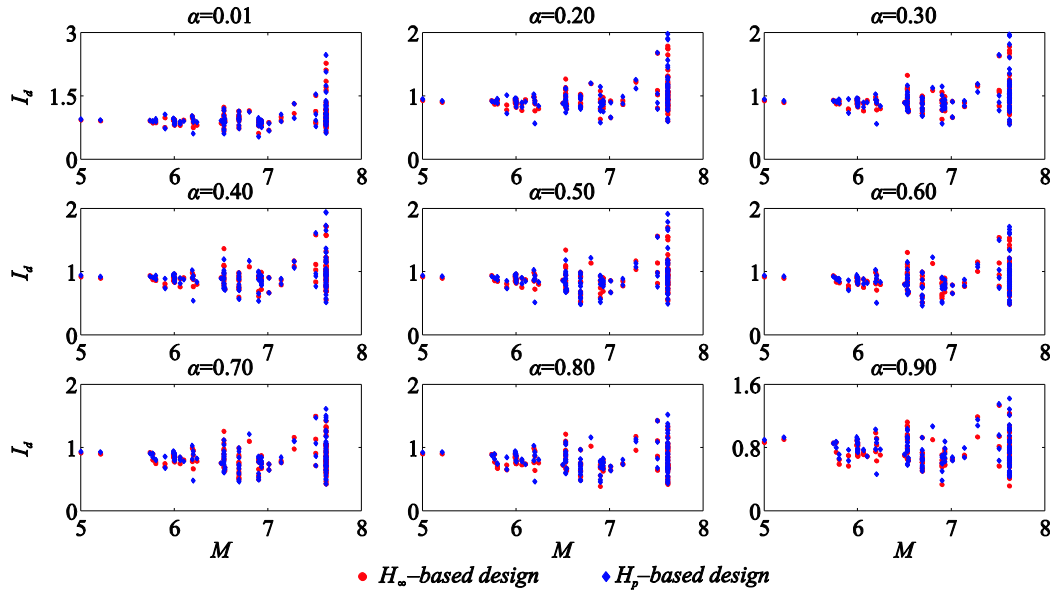


Fig. 6 Results for 8 DOF system ( $T_1=2.0289$  s): relationship between  $I_d$  and  $M$  for different values of  $\alpha$

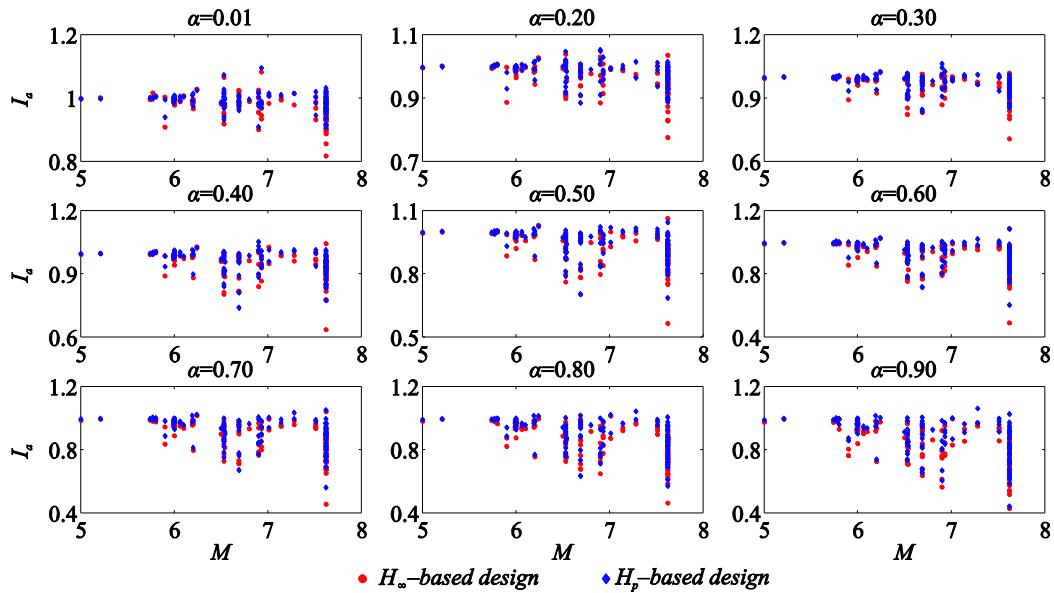


Fig. 7 Results for 8 DOF system ( $T_1=2.0289$  s): relationship between  $I_a$  and  $M$  for different values of  $\alpha$

This analysis clearly demonstrates that the seismic performance strongly depends on  $\alpha$ , i.e., enhanced performances are obtained when  $\alpha \rightarrow 1$ . When the nonlinear hysteretic component becomes negligible ( $\alpha=0.90$ ), the mean value of the index  $I_d$  is 0.6724 for  $\mu_{eff}=0.5693$  and 0.77072 for  $\mu_{eff}=0.1530$  ( $H_\infty$ -based design). The corresponding mean values of the index  $I_a$  are 0.68123 for  $\mu_{eff}=0.5693$  and 0.89892 for  $\mu_{eff}=0.1530$  ( $H_\infty$ -based design). This relationship between  $\alpha$  and the seismic performance is an expected result, because the nonlinear hysteretic component becomes

negligible with respect to the linear term when  $\alpha \rightarrow 1$ . Conversely, poor performances are found when  $\alpha \rightarrow 0$ . If  $\alpha = 0.01$ , then the mean value of the indexes  $I_d$  and  $I_a$  are significantly larger than 0.90 for most of the buildings. In this case, the dynamic characteristics of the structure changes drastically under the seismic motion and the TMD - designed by considering the initial linear elastic stiffness of the building - loses its efficacy. A significant variability of the indices can be observed, and it is also evident that the TMD designed according to either  $H_\infty$  or  $H_p$  methods can occasionally worsen the final performances.

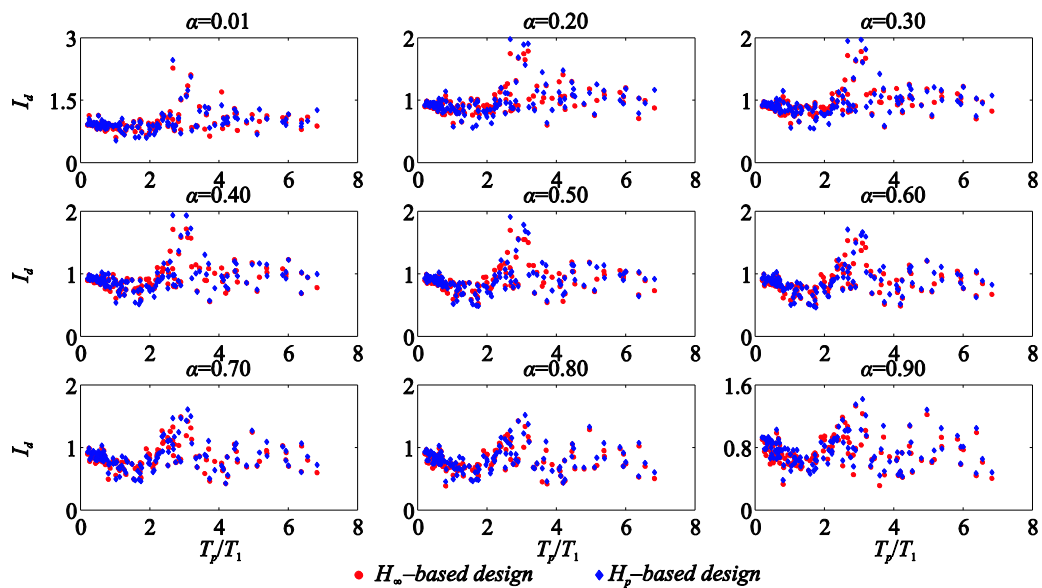


Fig. 8 Results for 8 DOF system ( $T_1=2.0289$  s): relationship between  $I_d$  and  $T_p/T_1$  for different values of  $\alpha$

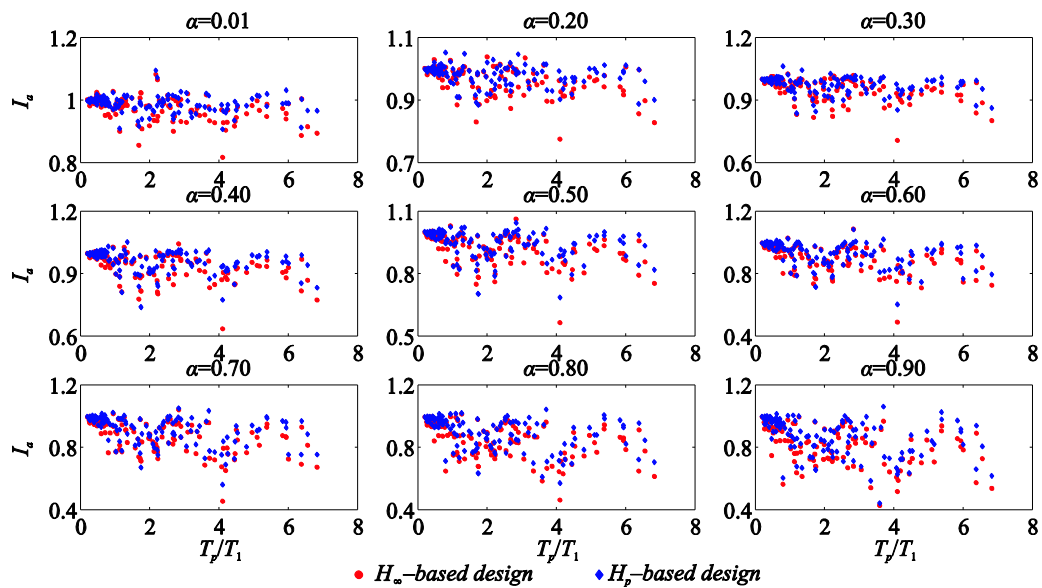


Fig. 9 Results for 8 DOF system ( $T_1=2.0289$  s): relationship between  $I_a$  and  $T_p/T_1$  for different values of  $\alpha$

It can be inferred from Fig. 14 that the average values of  $I_d$  and  $I_a$  are near to or less than 0.90 when the post-yield stiffness is greater than half of the initial stiffness. Below this threshold, the linear TMD designed according to  $H_\infty$  or  $H_p$  methods is likely to be ineffective for seismic control in the event of pulse-like ground motion and can result in a worsening of the structural performance. The increment of  $\mu_{eff}$  in the 4 DOF system is beneficial in reducing the displacements when  $\alpha \rightarrow 1$  whereas it is not advantageous when the post-yield stiffness is very small. On the other hand, it can be observed that a slight reduction of the floor acceleration is achieved for the highest

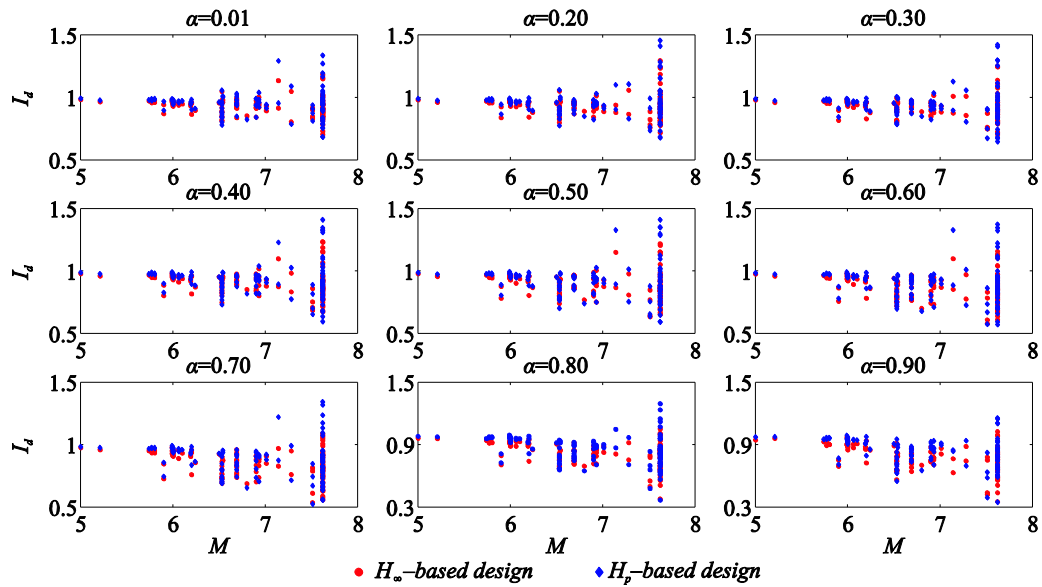


Fig. 10 Results for 16 DOF system ( $T_1=3.4687$  s): relationship between  $I_d$  and  $M$  for different values of  $\alpha$

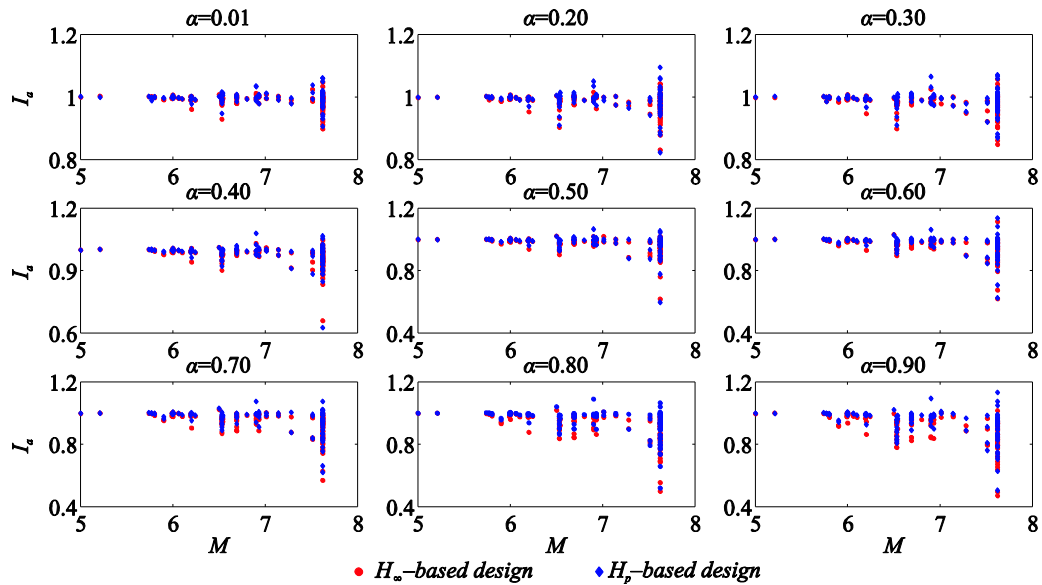


Fig. 11 Results for 16 DOF system ( $T_1=3.4687$  s): relationship between  $I_a$  and  $M$  for different values of  $\alpha$

value of  $\mu_{eff}$  ( $\mu_{ef}=0.5693$ ) even when the post-yield stiffness is near to be null (in this case, for  $\alpha=0.01$  the mean value of  $I_d$  is 0.90575 and the coefficient of variation is 0.0908). An increment of  $\mu_{eff}$  causes a reduction of the robustness, i.e., the standard deviation increases as  $\mu_{eff}$  increases. With the possible exception of the  $I_d$  values for 4 and 8 DOF systems, the smaller the mean value of the performance index, the larger its standard deviation. Finally, results in Fig. 14 also indicate that the  $H_\infty$  method leads to slightly superior TMD design solution with respect to the  $H_p$  method.

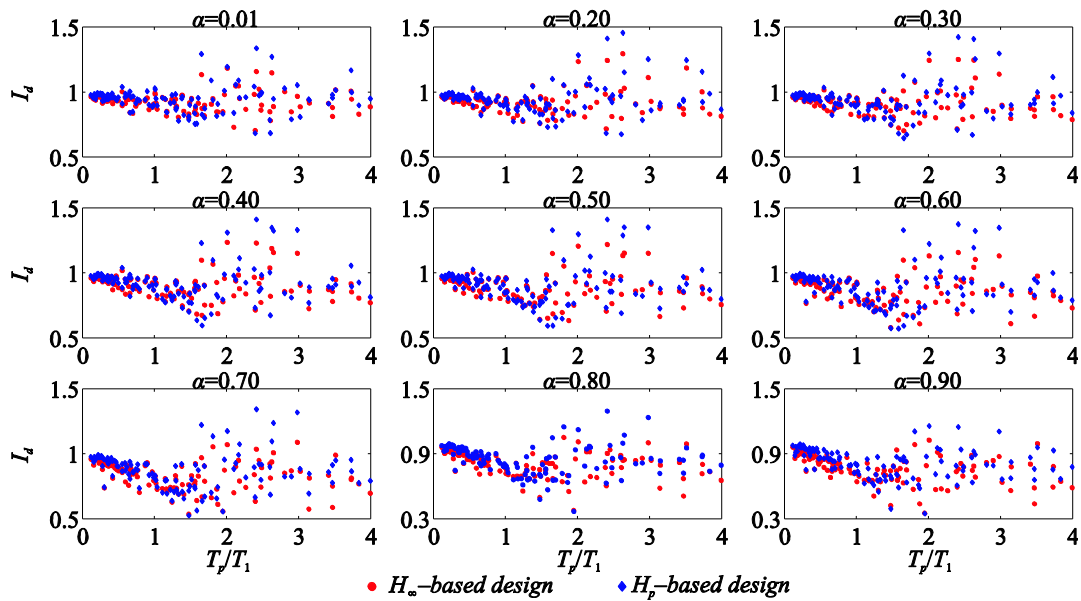


Fig. 12 Results for 16 DOF system ( $T_1=3.4687$  s): relationship between  $I_d$  and  $T_p/T_1$  for different values of  $\alpha$

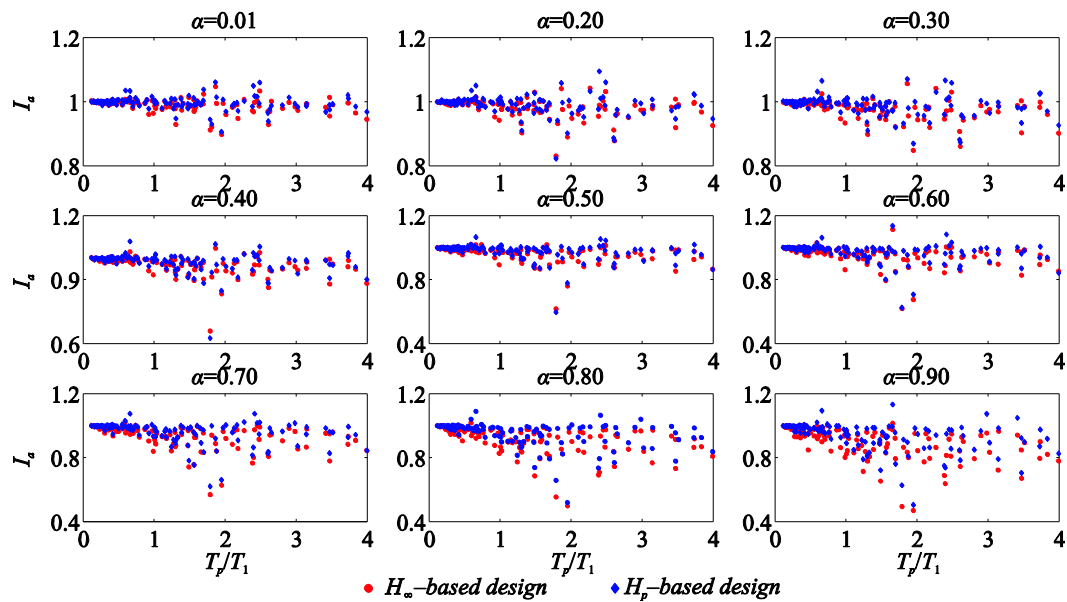


Fig. 13 Results for 16 DOF system ( $T_1=3.4687$  s): relationship between  $I_a$  and  $T_p/T_1$  for different values of  $\alpha$



displacement ratio of a linear elastic SDOF with and without TMD ranges from 0.75 to 0.95, whereas the coefficient of variation of this ratio ranges from 0.05 to 0.15 (when  $\mu_{eff}$  lies within 0.02 and 0.10). For a comparable structural system (the 16 DOF system with  $\alpha=0.90$  and  $\mu_{eff}=0.1530$ ), it is found that the mean value of  $I_d$  is 0.77072 and the coefficient of variation is about 0.17 under pulse-like ground motion. Therefore, no statistically significant differences can be identified. In agreement with (Sadek *et al.* 1997), the larger is the ratio between the TMD's mass and the mass of the protected system, the greater is the dispersion of the results. It is also convenient to compare the results for the 16 DOF system with those presented in (Lee *et al.* 2012) without taking into account the pulse-like characteristic of the seismic input, because some of the adopted values for  $\mu_{eff}$  are similar. For instance, the highest values of  $I_d$  when  $\alpha=0.90$  (i.e., the worst performance of a nearly linear system in terms of inter-storey drift) is about 1.2, which is close to the maximum value of the displacement-based performance index reported in (Lee *et al.* 2012) for a linear SDOF system (about 1.3). There are several differences between this study and the one presented in (Lee *et al.* 2012), such as the formulation of the performance index, the value of the fundamental period, and the residual hysteretic component of the response. However, it is likely that the most influential parameter be  $\mu_{eff}$  (the value considered in Lee *et al.* 2012 is equal to 0.05 and the value  $\mu_{eff}=0.1530$  adopted in this study results in enhanced average performances). Similar evidences between this study and the article by Lee *et al.* (2012) can be found for the 16 DOF system when  $\alpha=0.05$ . In this case, the highest value of  $I_d$  is about 1.4, in agreement with the maximum value of the displacement-based performance index shown in (Lee *et al.* 2012) for an approximate bilinear system having  $\alpha=0.05$ ,  $\mu_{eff}=0.05$  and  $T_1=2$  s. Statistical results for the 16 DOF and the 4 DOF nearly linear systems ( $\mu_{eff}=0.1530$  and  $\mu_{eff}=0.5693$ , respectively, with  $\alpha=0.90$ ) seem rather similar to that obtained by Matta (2013) for analogous (linear elastic) case studies.

### 3.5 Discussion

The considerations that can be formulated from this numerical study are listed in the following.

- An optimized linear TMD is effective in reducing inter-storey drift and floor acceleration due to pulse-like ground motion if the hypothesis of linear elastic behavior for the protected building is valid. In this case, the larger is  $\mu_{eff}$ , the greater is the effectiveness.
- The linear TMD designed by considering the elastic properties of the protected building is not effective if the structure exhibits a significant inelastic behaviour when subjected to near fault pulse-like ground motion. The average values of  $I_d$  and  $I_a$  are larger than 0.90 when the post-yield tangent stiffness is greater than one half of the initial stiffness.
- In contrast to what has been observed for linear protected buildings, the increment of  $\mu_{eff}$  is not recommended for displacement-control in the event of pulse-like ground motion when the post-yield stiffness is very small. This heavily worsens, both, the mean performance and the dispersions of the results. However, a large value of  $\mu_{eff}$  can be marginally beneficial for reducing structural accelerations when  $\alpha \rightarrow 0$ .
- There is a significant record-to-record variability. The larger is the ratio between TMD's mass and target mass of the protected system, the greater is the dispersion of the results. This holds true for, both, elastic and inelastic protected buildings. Occasionally, the linear TMD designed according to these methods can worsen the structural performance. A small value of the post-yield stiffness ( $\alpha \rightarrow 0$ ) can further aggravate negative structural performances. This indicates that the effectiveness of simplified TMD design procedures must be always validated through dynamic analyses conducted on a set of site-specific earthquake records. Attention should be paid in

determining the minimum size of the database used for the statistical assessment of the TMD design. The TMD's performance and the variability of the final results can result conflicting objectives. Hence, a robust design of the TMD may be appropriate in some circumstances, i.e., looking for the optimum parameters of the TMD in such a way that the average performance and its variability are minimized.

- The  $H_\infty$  method is preferable.

#### 4. Conclusions

This study provided a comprehensive assessment of some procedures to design linear TMD for inelastic structures subjected to pulse-like ground motion. These design procedures rely on the linear elastic properties of the protected structure. Two design methods (namely,  $H_\infty$  and  $H_p$  methods) have been compared and nonlinear dynamic analyses are performed for a set of 124 selected carefully natural earthquake records. Three shear-type structural systems with 4, 8 and 16 stories have been considered, with a fundamental period equal to 1.0783 s, 2.0289 s and 3.4687 s, respectively. The softening behavior is simulated by means of the Bouc-Wen model. The ratio between the TMD's mass and the mass of the last floor is 2. Therefore, the ratio of the TMD mass to the effective fundamental modal mass (denoted as  $\mu_{eff}$ ) varies between 0.1530 (for the 16 DOF system) and 0.5693 (for the 4 DOF system). Displacement- and acceleration-based performance indices have been examined, labeled as  $I_d$  and  $I_a$ , respectively.

It has been found that optimum design procedures for linear TMDs based on the elastic properties of the protected structural system are not effective for displacement-control of buildings that can undergo significant inelastic deformations when subjected to pulse-like ground motion, and they are marginally useful for acceleration mitigation. Occasionally, the TMD can worsen the structural performance and a small post-elastic stiffness can further aggravate negative seismic performances. The increment of the TMD's mass - which has been found useful in case of linear elastic protected buildings - has negative effects on the displacements of inelastic structures, slight positive consequences on the floor accelerations and it increases the dispersion of the results.

Finally, a note about the TMD's mass. In this study, the TMD mass has been assumed as twice the mass of the last floor. Such quite heavy mass cannot be mounted by using common building facilities available on the top floor. This mass value can be attained by exploiting roof gardens and helicopter platforms (when available). In doing so, large values of  $\mu_{eff}$  can be achieved in low- and middle-rise buildings, but this remains a very hard task for tall buildings. For multi-stories high-rise buildings, the opportunity of placing some isolators at one intermediate floor level can be considered: in this case, the stories below the isolators level constitute the protected building whereas the stories above the isolators level provide the TMD's mass (the behavior of the TMD depends on the isolator type). However, technical and economic benefits of such strategy with respect to a conventional base isolation system have to be determined.

In the future, the effectiveness of the TMD against pulse-like ground motion should be verified once its parameters are properly optimized for buildings with inelastic behaviors. The use of nonlinear TMDs is an area of future researches.

#### Acknowledgments

The research described in this paper was financially supported by the following project: “Sostenibilità sismica, tecnologica ed energetico ambientale negli interventi di riabilitazione/riuso sul patrimonio esistente: edifici strategici e ad uso pubblico”, Progetti di Ricerca Universitari Sapienza Università di Roma 2013.

## References

- Baker, J.W. (2007), “Quantitative classification of near-fault ground motions using wavelet analysis”, *Bull. Seismol. Soc. Am.*, **97**(5), 1486-1501.
- Bray, J.D. and Rodriguez-Marek, A. (2004), “Characterization of forward-directivity ground motions in the near-fault region”, *Soil Dyn. Earthq. Eng.*, **24**(11), 815-828.
- Chakraborty, S. and Roy, B.K. (2011), “Reliability based optimum design of tuned mass damper in seismic vibration control of structures with bounded uncertain parameters”, *Prob. Eng. Mech.*, **26**(2), 215-221.
- Hall, J.F., Heaton, T.H., Halling, M.W. and Wald, D.J. (1995), “Near source ground motion and its effects on flexible buildings”, *Earthq. Spectra*, **11**(4), 569-605.
- Hoang, N., Fujino, Y. and Warnitchai, P. (2008), “Optimal tuned mass damper for seismic applications and practical design formulas”, *Eng. Struct.*, **30**(3), 707-715.
- Ilkhouane, F. and Rodellar, J. (2007). *Systems with hysteresis - Analysis, identification and control using the Bouc-Wen model*, John Wiley & Sons.
- Ilkhouane, F., Hurtado, J.E. and Rodellar, J. (2007), “Variation of the hysteresis loop with the Bouc-Wen model parameters”, *Nonlinear Dyn.*, **48**(4), 361-380.
- Kalkan, E. and Kunnath, S.K. (2006), “Effects of fling-step and forward directivity on the seismic response of buildings”, *Earthq. Spectra*, **22**(2), 367-390.
- Kwok, K.C.S. and Samali, B. (1995), “Performance of tuned mass dampers under wind loads”, *Eng. Struct.*, **17**(9), 655-667.
- Lee, C.S., Goda, K. and Hong, H.P. (2012), “Effectiveness of using tuned-mass dampers in reducing seismic risk”, *Struct. Infrastruct. Eng.*, **8**(2), 141-156.
- Li, H.-J. and Hu, S.L.J. (2002), “Tuned mass damper design for optimally minimizing fatigue damage”, *J. Eng. Mech.*, **128**(6), 703-707.
- Lin, P.-Y., Lin, T.-K. and Hwang, J.-S. (2013), “A semi-active mass damping system for low- and mid-rise buildings”, *Earthq. Struct.*, **4**(1), 63-84.
- Lin, C.-C., Ueng, J.-M. and Huang, T.-C. (2000), “Seismic response reduction of irregular buildings using passive tuned mass dampers”, *Eng. Struct.*, **22**(5), 513-524.
- Liu, M.-Y., Chiang, W.-L., Hwang, J.-H. and Chu, C.-R. (2008), “Wind-induced vibration of high-rise building with tuned mass damper including soil-structure interaction”, *J. Wind Eng. Indust. Aerodyn.*, **96**(6-7), 1092-1102.
- Lukkunaprasit, P. and Wanitkorkul, A. (2001), “Inelastic buildings with tuned mass dampers under moderate ground motions from distant earthquakes”, *Earthq. Eng. Struct. Dyn.*, **30**(4), 537-551.
- Marano, G.C., Greco, R., Trentadue, F. and Chiaia, B. (2007), “Constrained reliability-based optimization of linear tuned mass dampers for seismic control”, *Int. J. Solid. Struct.*, **44**(22-23), 7370-7388.
- Marano, G.C. and Quaranta, G. (2009), “Robust optimum criteria for tuned mass dampers in fuzzy environments”, *Appl. Soft Comput.*, **9**(4), 1232-1243.
- Mavroeidis, G.P. and Papageorgiou, A.S. (2003), “A mathematical representation of near-fault ground motions”, *Bull. Seismol. Soc. Am.*, **93**(3), 1099-1131.
- Mollaioli, F., Bruno, S., Decanini, L. and Panza, G.F. (2006), “Characterization of the dynamical response of structures to damaging pulse-type near-fault ground motions”, *Meccanica*, **41**(1), 23-46.
- Mollaioli, F. and Bosi, A. (2012), “Wavelet analysis for the characterization of forward-directivity pulse-like ground motions on energy basis”, *Meccanica*, **47**(1), 203-219.
- Mollaioli, F., Liberatore, L. and Lucchini, A. (2014), “Displacement damping modification factors for pulse-

- like and ordinary records”, *Eng. Struct.*, **78**, 17-27.
- Matta, E. (2013), “Effectiveness of tuned mass dampers against ground motion pulses”, *J. Struct. Eng.*, **139**(2), 188-198.
- Pinkaew, T., Lukkunaprasit, P. and Chatupote, P. (2003), “Seismic effectiveness of tuned mass dampers for damage reduction of structures”, *Eng. Struct.*, **25**(1), 39-46.
- Sadek, F., Mohraz, B., Taylor, A.W. and Chung, R.M. (1997), “A method of estimating the parameters of tuned mass dampers for seismic applications”, *Earthq. Eng. Struct. Dyn.*, **26**(6), 617-635.
- Sgobba, M. and Marano, G.C. (2010), “Optimum design of linear tuned mass dampers for structures with nonlinear behavior”, *Mech. Syst. Sign. Proc.*, **24**(6), 1739-1755.
- Somerville, P.G. and Graves, R.W. (1993), “Conditions that give rise to unusually large long period ground motions”, *Proceedings of the Seminar on Seismic Isolation, Passive Energy Dissipation and Active Control, San Francisco: Applied Technology Council*, ATC17-1.
- Somerville, P.G., Smith, N.F., Graves, R.W. and Abrahamson, N.A. (1997), “Modification of empirical strong ground motion attenuation relations to include the amplitude and duration effects of rupture directivity”, *Seismol. Res. Lett.*, **68**(1), 199-222.
- Warburton, G.B. (1982), “Optimum absorber parameters for various combinations of response and excitation parameters”, *Earthq. Eng. Struct. Dyn.*, **10**(3), 381-401.
- Wu, J., Chen, G. and Lou, M. (1999), “Seismic effectiveness of tuned mass dampers considering soil-structure interaction”, *Earthq. Eng. Struct. Dyn.*, **28**(11), 1219-1233.

## Appendix A

A complete list of the pulse-like ground motion records considered in this study is given within Table A.1, together with the magnitude  $M$  and the pulse period  $T_p$  in [s].

Table A.1 Full list of pulse-like ground motion records together with the magnitude  $M$  and the pulse period  $T_p$  in [s]

Earthquake name	Year	$M$	$T_p$ [s]
Managua, Nicaragua-01	1972	6.24	1.90
Gazli, USSR	1976	6.80	4.87
Coyote Lake	1979	5.74	1.21
Imperial Valley-06	1979	6.53	4.03
Imperial Valley-06	1979	6.53	4.52
Imperial Valley-06	1979	6.53	3.35
Imperial Valley-06	1979	6.53	4.49
Imperial Valley-06	1979	6.53	7.36
Imperial Valley-06	1979	6.53	5.24
Imperial Valley-06	1979	6.53	4.61
Imperial Valley-06	1979	6.53	4.05
Imperial Valley-06	1979	6.53	3.84
Imperial Valley-06	1979	6.53	4.23
Imperial Valley-06	1979	6.53	5.39
Imperial Valley-06	1979	6.53	5.86
Imperial Valley-06	1979	6.53	4.80
Irpinia, Italy-01	1980	6.90	2.28
Westmorland	1981	5.90	2.43
Westmorland	1981	5.90	3.58
Coalinga-05	1983	5.77	0.69
Coalinga-05	1983	5.77	0.92
Coalinga-07	1983	5.21	0.40
Morgan Hill	1984	6.19	0.53
Morgan Hill	1984	6.19	1.24
N. Palm Springs	1986	6.06	1.55
N. Palm Springs	1986	6.06	1.38
San Salvador	1986	5.80	0.86
San Salvador	1986	5.80	0.96
Whittier Narrows-01	1987	5.99	0.79
Whittier Narrows-01	1987	5.99	0.95
Whittier Narrows-01	1987	5.99	0.76
Superstition Hills-02	1987	6.54	6.82
Superstition Hills-02	1987	6.54	2.28

Table A.1 Continued

Earthquake name	Year	$M$	$T_p$ [s]
Loma Prieta	1989	6.93	1.72
Loma Prieta	1989	6.93	2.32
Loma Prieta	1989	6.93	4.40
Loma Prieta	1989	6.93	4.47
Loma Prieta	1989	6.93	1.90
Erzican, Turkey	1992	6.69	2.65
Cape Mendocino	1992	7.01	2.55
Cape Mendocino	1992	7.01	3.00
Landers	1992	7.28	5.10
Landers	1992	7.28	7.50
Northridge-01	1994	6.69	3.53
Northridge-01	1994	6.69	3.53
Northridge-01	1994	6.69	2.21
Northridge-01	1994	6.69	1.65
Northridge-01	1994	6.69	1.04
Northridge-01	1994	6.69	2.41
Northridge-01	1994	6.69	0.50
Northridge-01	1994	6.69	1.23
Northridge-01	1994	6.69	3.48
Northridge-01	1994	6.69	3.49
Northridge-01	1994	6.69	3.11
Kobe, Japan	1995	6.90	0.95
Kobe, Japan	1995	6.90	2.06
Kobe, Japan	1995	6.90	2.73
Kobe, Japan	1995	6.90	1.43
Kobe, Japan	1995	6.90	1.62
Northwest China-03	1997	6.10	1.34
Kocaeli, Turkey	1999	7.51	10.91
Kocaeli, Turkey	1999	7.51	5.11
Kocaeli, Turkey	1999	7.51	5.87
Kocaeli, Turkey	1999	7.51	6.50
Chi-Chi, Taiwan	1999	7.62	2.63
Chi-Chi, Taiwan	1999	7.62	5.49
Chi-Chi, Taiwan	1999	7.62	2.12
Chi-Chi, Taiwan	1999	7.62	1.44
Chi-Chi, Taiwan	1999	7.62	4.77
Chi-Chi, Taiwan	1999	7.62	3.41
Chi-Chi, Taiwan	1999	7.62	6.45
Chi-Chi, Taiwan	1999	7.62	6.19

Table A.1 Continued

Earthquake name	Year	$M$	$T_p$ [s]
Chi-Chi, Taiwan	1999	7.62	8.61
Chi-Chi, Taiwan	1999	7.62	5.40
Chi-Chi, Taiwan	1999	7.62	6.96
Chi-Chi, Taiwan	1999	7.62	6.27
Chi-Chi, Taiwan	1999	7.62	9.11
Chi-Chi, Taiwan	1999	7.62	8.58
Chi-Chi, Taiwan	1999	7.62	11.83
Chi-Chi, Taiwan	1999	7.62	13.29
Chi-Chi, Taiwan	1999	7.62	8.49
Chi-Chi, Taiwan	1999	7.62	12.94
Chi-Chi, Taiwan	1999	7.62	10.47
Chi-Chi, Taiwan	1999	7.62	12.92
Chi-Chi, Taiwan	1999	7.62	13.84
Chi-Chi, Taiwan	1999	7.62	8.36
Chi-Chi, Taiwan	1999	7.62	12.02
Chi-Chi, Taiwan	1999	7.62	7.27
Chi-Chi, Taiwan	1999	7.62	8.31
Chi-Chi, Taiwan	1999	7.62	5.74
Chi-Chi, Taiwan	1999	7.62	12.17
Chi-Chi, Taiwan	1999	7.62	5.15
Chi-Chi, Taiwan	1999	7.62	3.98
Chi-Chi, Taiwan	1999	7.62	9.18
Chi-Chi, Taiwan	1999	7.62	9.04
Chi-Chi, Taiwan	1999	7.62	7.55
Chi-Chi, Taiwan	1999	7.62	10.04
Chi-Chi, Taiwan	1999	7.62	9.72
Chi-Chi, Taiwan	1999	7.62	8.26
Chi-Chi, Taiwan	1999	7.62	12.03
Chi-Chi, Taiwan	1999	7.62	7.85
Chi-Chi, Taiwan	1999	7.62	6.75
Chi-Chi, Taiwan	1999	7.62	5.43
Chi-Chi, Taiwan	1999	7.62	10.89
Chi-Chi, Taiwan	1999	7.62	9.01
Chi-Chi, Taiwan	1999	7.62	10.33
Chi-Chi, Taiwan	1999	7.62	4.30
Chi-Chi, Taiwan-03	1999	6.20	3.19
Chi-Chi, Taiwan-03	1999	6.20	1.35
Chi-Chi, Taiwan-03	1999	6.20	0.91
Duzce, Turkey	1999	7.14	5.57

Table A.1 Continued

Earthquake name	Year	$M$	$T_p$ [s]
Duzce, Turkey	1999	7.14	5.72
Yountville	2000	5.00	0.73
Bam, Iran	2003	6.50	2.04
Parkfield	2004	6.00	1.33
Parkfield	2004	6.00	1.15
Parkfield	2004	6.00	1.02
Parkfield	2004	6.00	0.69
Parkfield	2004	6.00	1.42
Parkfield	2004	6.00	1.27
Parkfield	2004	6.00	1.20
Parkfield	2004	6.00	0.56
Parkfield	2004	6.00	0.50
Parkfield	2004	6.00	0.62